



## **Autophagy, SMAD-1, and apoptotic pathways are correlated with L-carnitine protective effect against dexamethasone-induced osteoporosis in Wistar rats**

*Sanaa A. Ahmed\*, Dalia A. Elbahi*

*Department of Pharmacology, Faculty of Medicine, Sohag University, Sohag 82524, Egypt*

### **Abstract**

Osteoporosis (O.P) is a metabolic bone disease characterized by bone mass loss and bone weakness. The cofactor in fatty acid beta-oxidation, L-carnitine (L-C), has been found to regulate osteoblast activity. Therefore, this work aimed to investigate the potential defensive properties of L-C versus dexamethasone (DEXA) induced O.P, as well as the underlying mechanisms. Thirty female Wistar rats were divided randomly into three equal groups (n = 10). The control group: received saline throughout the study; the DEXA-treated group: received DEXA (7 mg/kg/week) I.M. for four successive weeks; the L-C + DEXA treated group: received L-C (100 mg/kg/day, orally) for two weeks followed by L-C+ DEXA for a further four successive weeks simultaneously in the same previous doses and routes. L-C treatment attenuated the decline in femur and body weights, calcium, osteoprotegerin (OPG), and total antioxidant capacity resulting from DEXA administration. In contrast, L-C ameliorated DEXA-induced elevation in alkaline phosphatase and oxidative stress. Furthermore, L-C reduced the expression of an apoptosis-related gene; caspase-3, however, augmented the expression of autophagy-related genes ATG-5 and Smad-1 in rat bone. Histopathological findings further supported the protective effects of LC against DEXA-induced O.P. In conclusion, the current study findings demonstrated the protective effects of L-C on DEXA-induced O.P due to the reduction of oxidative stress, apoptosis, and increasing autophagy and smad-1 protein gene expression. Consequently, L-C can be used as an additive in the treatment of O.P.

**Keywords:** Apoptosis; Autophagy; Bone mineral density; Osteoporosis; Osteoprotoren; L-carnitine.

**Received on: 15. 07. 2022**

**Revised on: 27. 07. 2022**

**Accepted on: 28. 07. 2022**

\*Correspondence Author:

Fax: +201009299606

E-mail address:

[sanaa\\_ahmed@med.sohag.edu.eg](mailto:sanaa_ahmed@med.sohag.edu.eg)

### **1. Introduction**

Osteoporosis (O.P) is a chronic metabolic bone disease that primarily affects postmenopausal women and the elderly, and it presents a severe health risk (Castelo-Branco, 1998). Bone mass is determined by bone remodeling, which is mediated by osteoblastic and osteoclastic cells (Zhang et al., 2009). However, remodeling activity is accelerated

in postmenopausal women, and production rates are slower than resorption, resulting in O.P (Clarke & Khosla, 2010). Several mechanisms influence bone remodeling, including the interaction of systemic hormones, cytokines, growth factors, and transcription factors in addition to the osteoblastic and osteoclastic cell lineages (Raisz, 2005). However, changes in reactive

oxygen species (ROS) and antioxidant systems appear to be involved in the pathophysiology of bone loss (Domazetovic et al., 2017). ROS induces apoptosis in osteoblasts and osteocytes, promoting osteoclastogenesis (Baek et al., 2010). Several studies have also revealed that osteoprotegerin (OPG), a soluble decoy receptor of receptor activator of nuclear-factor-kappa-B (RANKL), negatively regulates osteoclast differentiation and bone resorption (Cawley et al., 2020).

Different osteogenic signaling molecules, such as bone morphogenetic protein-2 (BMP2) and fibroblast growth factor-2 (FGF2), influence osteoblast differentiation (Jiang et al., 2015) and have been reported to be mediated by the activation of transcriptional factor; SMAD family members (Smad)-1, 5, and 8 upon ligand binding which is essential for BMP2-induced osteoblastic differentiation (Langenfeld et al., 2006; Ding et al., 2018). Particularly in highly differentiated cells like myocytes, osteocytes, and neurons, autophagy plays a critical role in maintaining cell homeostasis (Mizushima & Levine, 2010; Galati et al., 2019). The rate of autophagy accelerates under various stress circumstances to support the recycling of cytoplasmic components and cell viability (Li et al., 2018). Approximately 20 members of the autophagy-related genes (ATG) family of highly conserved genes control autophagy (Montaseri et al., 2020).

Current clinical agents that stimulate bone formation and/or inhibit bone resorption are effective in preventing and treating O.P. However, most of their side effects are too severe, such as increased risks of esophagitis, nausea, and abdominal pain (Abrahamsen, 2010), thromboembolic events, vaginal bleeding, and endometrial, breast, and ovarian cancers (Beral, 2007; Liu et al., 2019). consequently, it is critical to investigate and create natural products that are useful in preventing or treating O.P while also interpreting their mechanisms of action. Therefore, finding new therapeutic strategies for postmenopausal O.P with fewer side effects is necessary.

Human osteoblast functions and intracellular calcium signaling have been discovered to be promoted by L-carnitine (L-C), a mediator in fatty acid beta-oxidation and a carrier for acetyl groups through the mitochondrial membrane (Colucci et al., 2005; Pekala et al., 2011; Ferraretto et al.,

2018). In rats, L-C was found to have antioxidant activity, which helped to prevent age-related mitochondrial dysfunction (Bernard et al., 2008). By improving mitochondrial performance, L-C may have a beneficial effect on high-energy-demanding organs like bone and muscle (Marcovina et al., 2013). This study may aid in clarifying the mechanisms that underlie L-C's benefit on bone cells, allowing L-C to be used in the treatment of bone fragility in the elderly.

## 2. Materials and Methods

### 2.1. Animals

Thirty female Wistar rats 33-35 weeks old, weighing 200-250 grams. were purchased from the Animal House at Sohag University's Faculty of Medicine and housed at a room temperature of 22-28°C. All animals were fed a standard pellet diet and subjected to periodic light/dark cycles. In addition, they were given food and water *ad libitum*. The experimental protocol was approved by the Scientific Research Ethical Committee Faculty of Medicine Sohag University, Egypt, with approval No. 5/13/2021/01, according to the European Community guidelines (2010/63/EU) for the care and use of laboratory animals.

### 2.2. Drugs and chemicals

Dexamethasone (DEXA) was obtained from Biotech Pharmaceutical Co., Ltd. Egypt; 35 mg were dissolved in 25 mL saline (1.4 mg/ mL). While Sigma Aldrich Industry in England provided L-C. 1 g of L-C was dissolved in 10 mL distilled water (100 mg/ mL). The drugs were prepared on the same day of treatment. Serum levels of calcium, and alkaline phosphatase (ALP), were measured by kits obtained from Human Gesellschaft fur Biochemica und Diagnostica mbH. Germany. Serum level of inorganic phosphorous was measured using kits obtained from Spectrum Diagnostic Egyptian Company for Biotechnology (S.A.E), Egypt. Total antioxidant capacity (TAC) was measured utilizing kits purchased from Biodiagnostic Company Pharmaceutical Industries, Egypt. While ELISA kits for estimation of osteoprotegerin (OPG) were purchased from SinoGeneclon Biotech Co., Ltd. China.

### 2.3. Experimental design

The thirty Wistar rats were divided randomly into three groups, ten animals each. The first group

(control group): received 1 mL of distilled water orally as a vehicle daily for the entire experiment period. The second group (DEXA-treated group): For two weeks, rats were given saline intramuscularly (I.M.) once a week, then treated with DEXA (7 mg/kg) I.M which was dissolved in saline once a week for four sequential weeks. (Lucinda et al., 2010). The third group (L-C + DEXA treated group): received L-C 100 mg/kg/day orally (Moustafa & Boshra, 2011) for two weeks followed by L-C (100 mg/kg/day orally) and DEXA (7 mg/ kg /week I.M) simultaneously for a further four consecutive weeks.

## 2.4. Sample extraction

### 2.4.1. Preparation of serum

The rats were euthanized by decapitation under diethyl ether, and blood from neck veins was taken in pre-labeled centrifuge tubes at the end of the experiment. The tubes were centrifuged for 15 minutes at 3500 rpm in a Heraeus Sepatech centrifuge (Labofuge 200, DJB Lab care Co). Serum was isolated and preserved immediately at -20 °C until analysis.

### 2.4.2. Collection of bone samples

Each animal's femurs and tibias were cautiously dissected and cleaned from adjacent muscles. The weight and length of the right femur were measured then covered with saline gauze to preserve their moisture and kept at -20 °C for bone mineral density (BMD) and bone mineral content (BMC) evaluation. The right tibia was weighted and immersed in liquid nitrogen and homogenized for 5 min in frozen phosphate buffer saline (0.01 M, pH 7.4;20% w/v) by Gals-Col, LLC USA motor-driven homogenizer followed by centrifugation at 10000 r.p.m at -4 °C for 30 min and supernatant were collected for biochemical analysis. For histopathological evaluation, left femurs were rapidly fixed in 10% neutral buffered formaldehyde. The left tibias were submerged in liquid nitrogen and then maintained at -80 °C to isolate the RNA gene of caspase 3, Smad-1, and ATG-5.

## 2.5. Estimation of Seedor index

It was estimated by measuring the femur weight, in (mg) using digital balance, and its length in (mm) from the medial condyle to the femoral head using a digital caliper (Seedor et al., 1991).

$$\text{Seedor Index} = \frac{\text{Femur Weight (mg)}}{\text{Femur length (mm)}}$$

## 2.6. Biochemical examination

### 2.6.1. Calcium and phosphorus concentration

Diagnostic chemical kits were used to estimate calcium and phosphorous serum concentrations using Spectrophotometer (5010) Robert Riele GmbH & Co KG, Berlin Germany. They were employed in accordance with the manufacturer's guidelines, and the absorbance variations were calculated at 546 nm and 340 nm, respectively, as reported by Daly & Ertingshausen (1972) and Barnett et al. (1976).

### 2.6.2. Alkaline phosphatase (ALP) activity

Diagnostic biochemical analyses were utilized for the assessment of of ALP serum activity in accordance with the manufacturer recommendations which are based on the ability of ALP to convert the para-Nitrophenyl phosphate (p-NPP) to para-nitrophenol at alkaline pH and the alteration of absorption of the colored product was assessed at a wavelength of 405 nm.

### 2.6.3. Estimation of bone lipid peroxidation and nitric oxide (NO) levels

MDA and NO levels in bone were determined by a colorimetric method according to Ohkawa et al. (1979) and Montgomery (1961), respectively. MDA assessment depends on the reaction of a chromogenic reagent, N-methyl-2- phenylindole to MDA to generate a stable chromophore, with the alterations of absorbance measured at 534 nm. The method of NO depends on the formation of nitrous acid diazotize sulphanilamide combined with N-(1-naphthyl) ethylenediamine in the presence of nitrite and acid environment. At 540 nm, changes in absorbance were evaluated.

### 2.6.4. Bone total antioxidant capacity (TAC) status

TAC status in the bone homogenate was determined colorimetrically by an enzymatic reaction according to manufacturer instructions. TAC is calculated by combining the sample's antioxidants with a known amount of exogenous hydrogen peroxide (H<sub>2</sub>O<sub>2</sub>). An enzymatic reaction manufacturers' recommendations, template cDNA

involved in the conversion of 3,5 dichloro-2-hydroxy benzenesulfonate to a colorful product that measures the remaining H<sub>2</sub>O<sub>2</sub> (Koracevic et al., 2001).

### 2.6.5. Osteoprotegerin (OPG)

The ELISA (enzyme-linked immunosorbent test) kits were applied to detect OPG concentration in bone tissue. It was measured in accordance with the manufacturer's specifications. The following is a brief description of the method: Pipette 50 µl of the standard or a sample that has been diluted five times into the testing standard and sample wells., followed by incubation for 30 minutes at 37°C. The procedure was recurring five times at 30-second intervals. Each well received 50 µl of Horseradish Peroxidase (HRP-conjugate reagent), followed by chromogen solutions A and B, and finally a stop solution. Microplate reader Stat fax 2600 was used to calculate absorbance at 450 nm (Awareness Technologies, Palm City, USA) (Samelson et al., 2008).

### 2.7. Bone mineral density (BMD) and bone mineral content (BMC) evaluation

Each right femur is kept at -20 °C. The bones were moistened after being defrosted at room temperature and immersed in a saline solution for measuring BMD and BMC using a Norland XR 46, version 3.9.6/2.3.1 (USA) dual-energy x-ray absorptiometry instrument fitted with specific software for small animal examinations. The experimental animals' femurs were scanned with a resolution of 1.0 x1.0 mm and a scan speed of 60 mm/s.

### 2.8. Estimation of Caspase-3, Smad-1, and ATG-5 gene expression with Real time-quantitative PCR (RT-qPCR) analysis

The left tibia was dissected and quickly frozen in liquid nitrogen, and the bone tissues were crushed into a powder with a pestle to preserve the RNA. Following the manufacturer guidelines, the whole RNA was isolated from bone tissue using the RNeasy Mini Kit (Qiagen, USA). A spectrophotometer (Biotech Nanodrop, USA) was used to assess the purity and amount of the RNA fraction in each sample. According to the

was constructed applying a High-Capacity cDNA. Reverse Transcription Kit (Thermo Scientific Fisher, USA). Table 1 shows the nucleotide sequences of the forward and reverses primers. The amplification was carried out on an Applied Biosystems 7500 device (USA). Following a 5-minute denaturation at 95°C, 40 cycles of denaturation at 95°C for 20 seconds, annealing at 60°C for 30 seconds, and extension at 72°C for another 30 seconds were performed. The relative fold changes in gene expression were computed using the 2<sup>-ΔΔ</sup> CT comparative method, with the target gene expression levels normalized to β-actin as a housekeeping gene (Schmittgen & Livak, 2008).

### 2.9. Histopathological Examination

Femurs were immediately fixed in 10% neutral buffered formaldehyde for 24 hours. The bones were gradually decalcified by soaking them in 5% nitric acid until they softened. Upgrading alcohol concentrations (50 % to 100 %) was used to dry the bones before they were implanted in Paraffin. The femoral diaphysis was sliced into 4 µm thick longitudinal sections parallel to the long axis of the bones. Deparaffinization in two changes of xylene (20 minutes each) before rehydration in downgraded alcohol (100% through 50%) was done. The slices were rinsed with water and then stained with Mayer's hematoxylin and eosin (H&E stain). Finally, the sections were mounted using DPX (Dibutylphthalate Polystyrene Xylene) reagent and then inspected using the Olympus (model CX21) Japan Light microscope (Suvarna et al., 2018).

### 2.10. Statistical analysis

The commercially available statistical analysis software (IBM-SPSS version 25.0) was used for data evaluation. The graphs were formed using GraphPad Prism software version 9. 3. 1 (471) (GraphPad Software, LLC, San Diego, CA, USA). The Shapiro-Wilk test was used to determine whether data were normally distributed. Variables were summarized as mean ± standard error of the mean (SEM). For multiple comparisons, a one-way ANOVA was employed, followed by Tukey's post hoc test. The differences were considered significant if p < 0.05.

**Table 1: Forward and reverse primer sequences for target genes**

Gene	(Primer sequence) 5'-3'	Product size/bp
Caspase-3	Forward: CAGAGCTGGACTGCGGTATTGA Reverse: AGCATGGCGCAAAGTGACG	NM_012922.2 172
Smad-1	Forward: TCAATAGAGGAGATGTTCAAGCAGT Reverse: AAACCATCCACCAACACGCT	NM_013130.3 133
ATG- 5	Forward: TTGAATATGAAGGCACACCACTGAA Reverse: GCATCCTTAGATGGAGAGTGCAGA	NM_001014250.1 151
Beta-actin	Forward: GTCCACCCGCGAGTACAAC Reverse: GGATGCCTCTCTTGCTCTGG	NM_031144.3 260

### 3. Results

#### 3.1. Effect on femur and body weights

According to **Table 2**, there is a substantial decrease ( $P < 0.001$ ) in femur weight after four weeks of DEXA treatment compared to the control. Nevertheless, simultaneous administration of L-C (L-C +DEXA) significantly elevated ( $P < 0.001$ ) the weight of the femur compared to the DEXA group. In contrast, DEXA administration induced a substantial reduction ( $P = 0.01$ ) in body weight compared to the control group, and concomitant L-C administration significantly increased ( $P = 0.035$ ) body weight compared to the DEXA-treated group.

#### 3.2. Seedor Index

DEXA treated group exhibited a marked decrease ( $P < 0.001$ ) in Seedor index compared to the control group. Additionally, the supplementation of L-C to DEXA induced a significant elevation ( $P < 0.001$ ) in the Seedor index compared to the DEXA treated group as depicted in **Table 2**.

#### 3.3. Effect on serum calcium and phosphorous levels

As illustrated in **Table 3**, DEXA treatment for four weeks led to significantly decreased calcium and elevated phosphorous levels ( $P < 0.001$ ). However, L-C administration caused a significant increase in calcium and a reduction ( $P < 0.001$ ) in phosphorous concentrations compared to the DEXA group.

#### 3.4. Effect on serum alkaline phosphatase (ALP) activity

**Table 3** shows that DEXA administration encouraged a considerable elevation ( $P < 0.001$ ) of ALP activity, on the contrary, L-C administration

concomitant to DEXA ameliorated this effect and induced a significant decrease ( $P < 0.001$ ) in ALP activity.

#### 3.5. Effect on MDA and NO concentrations

As depicted in **Table 4**, DEXA administration induced a valuable elevation ( $P < 0.001$ ) in bone tissue concentrations of MDA and NO in comparison to the control group. In contrast, rats supplemented with L-C in addition to the DEXA (L-C+ DEXA) group demonstrated a substantial decrease in MDA ( $P < 0.0001$ ) and NO ( $p = 0.012$ ) compared to the DEXA-treated group.

#### 3.6. Effect on the concentration of total antioxidant (TAC) status

Compared to the control groups, DEXA treatment resulted in a substantial reduction ( $p < 0.0001$ ) in bone TAC levels. In contrast to DEX-treated groups, L-C administration along with DEXA demonstrated a substantial elevation ( $p < 0.0001$ ) in TAC levels, as depicted in **Figure 1**.

#### 3.7. Effect on osteoprotegerin (OPG) concentration

According to **Figure 2**, DEXA supplementation brought a marked decrease ( $P < 0.0001$ ) in the bone concentration of OPG compared to the control group. In contrast, administration of L-C in addition to the DEXA (L-C+ DEXA) group demonstrated a significant elevation in OPG ( $P < 0.0001$ ) compared to the DEXA-treated group.

#### 3.8. Measurement of BMD and BMC by Dual-energy X-ray absorptiometry

Compared to the control group, the administration of DEXA to the experimental group resulted in a

**Table 2. Effect of L-C administration on femur weight, body weight, and seedor index in DEXA-induced osteoporosis in Wistar rats.**

Groups	Control	DEXA	L-C + DEXA
<b>Femur weight (mg)</b>	1080.30 ±29.83	663.40±21.83 ( <i>P</i> =0.000) <sup>a</sup>	980.40±31.27 ( <i>P</i> =0.000) <sup>b</sup>
<b>Body weight (g)</b>	247.98 ±7.24	209.10 ±5.07 ( <i>P</i> =0.01) <sup>a</sup>	242.80 ± 4.94 ( <i>P</i> =0.035) <sup>b</sup>
<b>Seedor Index</b>	31.04±0.87	19.37±0.63 ( <i>P</i> =0.000) <sup>a</sup>	28.21±0.78 ( <i>P</i> =0.000) <sup>b</sup>

Values were demonstrated as the mean ± SEM (n = 10). values were analyzed by one-way ANOVA, then a post hoc analysis. *P* < 0.05 was established as significant. <sup>a</sup> significant vs. control, <sup>b</sup> significant vs. DEXA group. L-C: L-Carnitine. DEXA: dexamethasone.

**Table 3. Effect of L-C administration on serum calcium, phosphorous, and alkaline phosphatase (ALP) levels in DEXA-induced osteoporosis in Wistar rats.**

Groups	Control	DEXA	L-C + DEXA
<b>Serum calcium (mg/dl)</b>	10.95±0.07	8.05±0.14 ( <i>P</i> =0.000) <sup>a</sup>	10.23±0.23 ( <i>P</i> =0.000) <sup>b</sup>
<b>Serum phosphorous (mg/dl)</b>	6.54±0.08	8.77±0.20 ( <i>P</i> =0.000) <sup>a</sup>	7.11±0.14 ( <i>P</i> =0.000) <sup>b</sup>
<b>Serum ALP (U/L)</b>	160.90±4.38	350.40± 8.82 ( <i>P</i> =0.000) <sup>a</sup>	179.90±2.92 ( <i>P</i> =0.000) <sup>b</sup>

Values were demonstrated as the mean ± SEM (n = 10). values were analyzed by one-way ANOVA, then a post hoc analysis. *P* < 0.05 was established as significant. <sup>a</sup> significant vs. control, <sup>b</sup> significant vs. DEXA group. L-C: L-Carnitine. DEXA: dexamethasone.

**Table 4. Effect of L-C administration on MDA and NO in DEXA-induced osteoporosis in Wistar rats.**

	Control	DEXA	L-C + DEXA
<b>Bone MDA (nmol/ml)</b>	363.04 ±8.78	470.69 ±14.45 ( <i>P</i> =0.000) <sup>a</sup>	400.69 ±5.50 ( <i>P</i> =0.000) <sup>b</sup>
<b>Bone NO (µmol/L)</b>	193. 26 ±5.08	233.83 ±5.18 ( <i>P</i> =0.000) <sup>a</sup>	210.54 ±5.69 ( <i>P</i> =0.012) <sup>b</sup>

Values were demonstrated as the mean ± SEM (n = 10). values were analyzed by one-way ANOVA, then a post hoc analysis. *P* < 0.05 was established as significant. <sup>a</sup> significant vs. control, <sup>b</sup> significant vs. DEXA group. L-C: L-Carnitine. DEXA: dexamethasone. MDA: malondialdehyde. NO: nitric oxide.

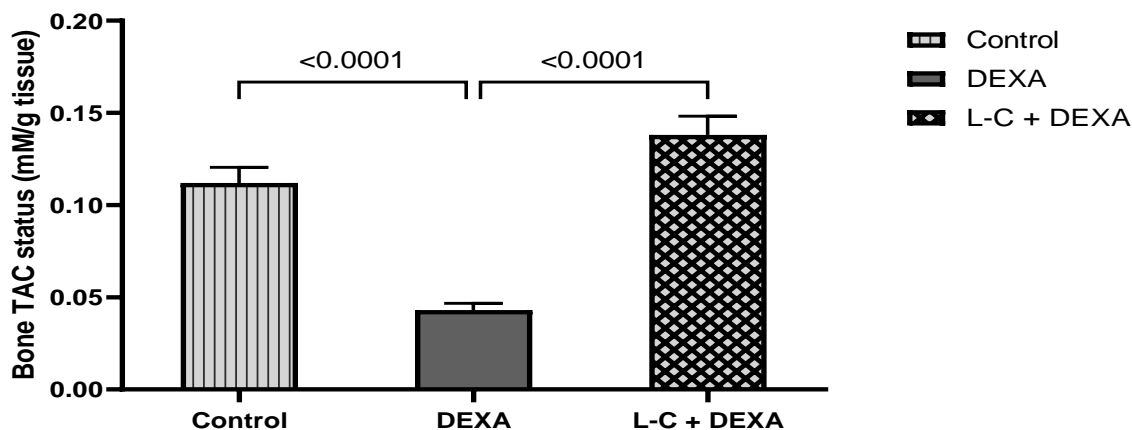


**Figure 1.** Effect of L-C administration on bone total antioxidant capacity status (TAC) in DEXA-induced osteoporosis in Wistar rats. Values were demonstrated as the mean  $\pm$  SEM (n = 10). values were analyzed by one-way ANOVA, then Tukey's post hoc analysis. P < 0.001 was established as significant. DEXA. L-C: L-Carnitine. DEXA: dexamethasone.

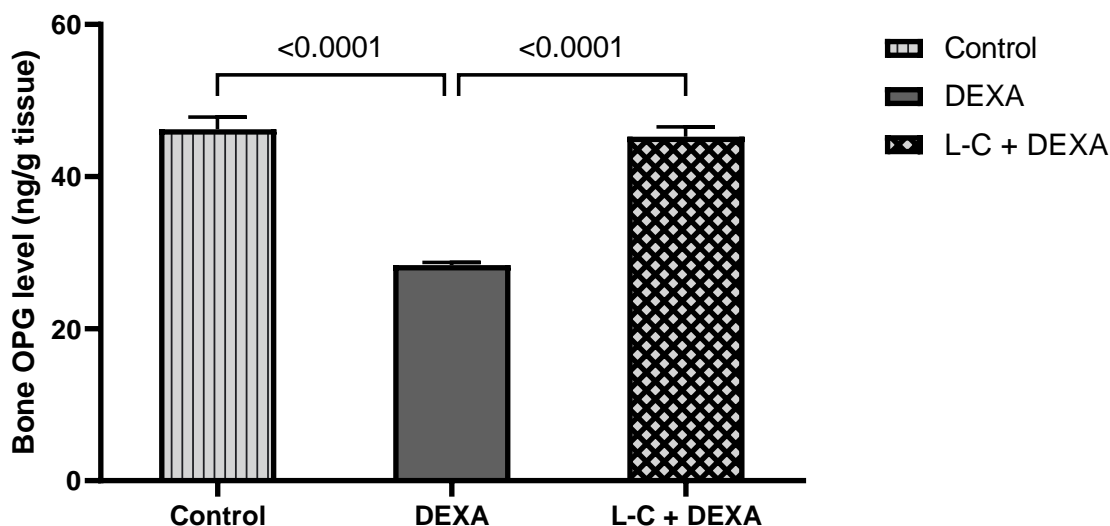


**Figure 2.** Effect of L-C administration on the bone concentration of osteoprotegerin (OPG) in DEXA-induced osteoporosis in Wistar rats. Values were demonstrated as the mean  $\pm$  SEM (n = 10). values were analyzed by one-way ANOVA, then Tukey's post hoc analysis. P < 0.001 was established as significant. DEXA. L-C: L-Carnitine. DEXA: dexamethasone.

substantial decrease (P<0.0001) in both BMD and BMC. Moreover, the addition of L-C (L-C + DEXA) resulted in a valuable rise (P<0.0001) in both previous measures compared to the DEXA treated group as shown in **Figures 3 and 4**.

### 3.9. Effect on caspase-3 gene expression

As shown in **Figure 5**, DEXA administration for four weeks resulted in significant advancement in caspase-3 mRNA expression (P < 0.0001) compared to the control group. Nevertheless, simultaneous administration of L-C with DEXA (L-C + DEXA) gave rise to a significant restoration (P

= 0.028) of caspase-3 mRNA expression levels compared to the DEXA group.

### 3.10. Effect on Smad-1 gene expression

**Figure 6** demonstrates that in comparison to DEXA treated group, the mRNA expression of Smad-1 decreased, with a statistically significant difference (P<0.0001). However, the mRNA expression of Smad-1 was statistically significantly increased (P<0.0001) after simultaneous treatment with L-C (L-C +DEXA) compared to the DEXA-treated group.

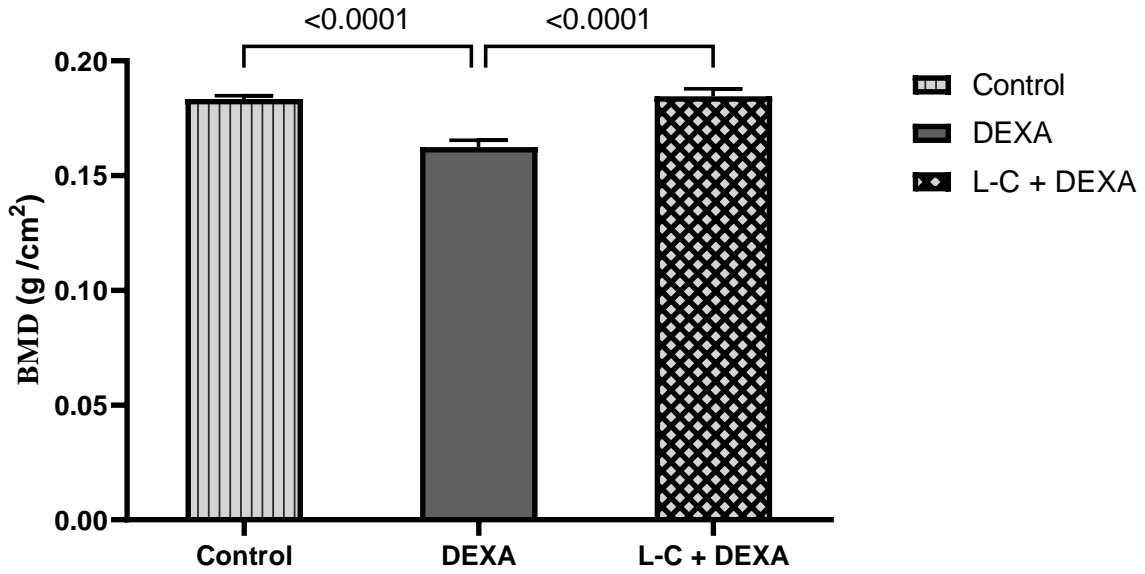


**Figure 3.** Effect of L-C administration on bone mineral density (BMD) in DEXA-induced osteoporosis in Wistar rats. Values were demonstrated as the mean  $\pm$  SEM (n = 10). values were analyzed by one-way ANOVA, then Tukey's post hoc analysis. P < 0.001 was established as significant. DEXA. L-C: L-Carnitine. DEXA: dexamethasone.

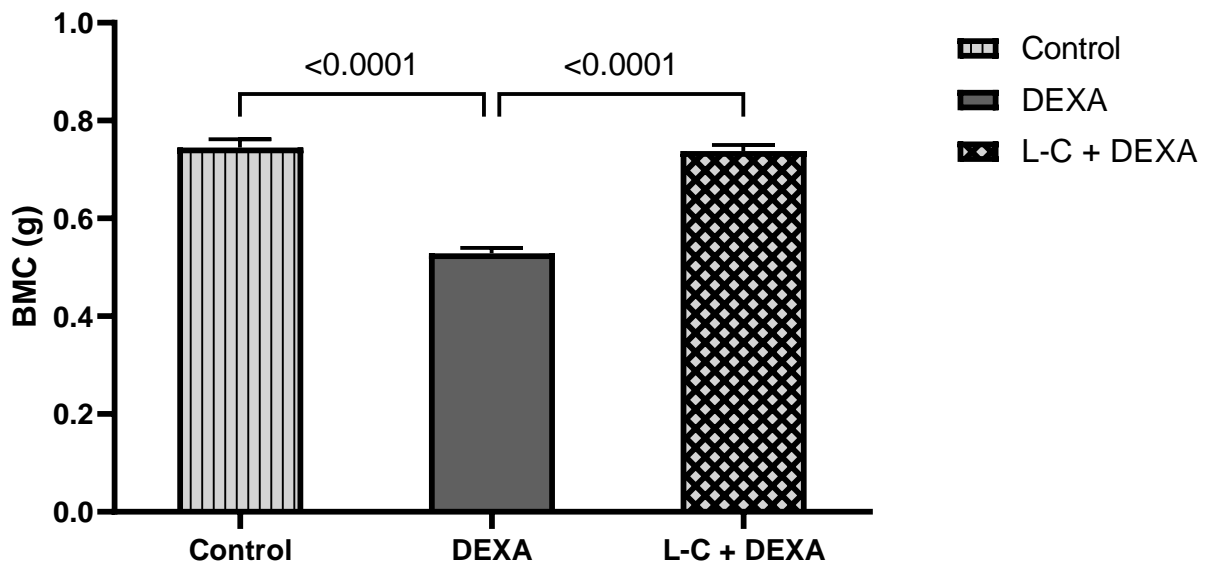


**Figure 4.** Effect of L-C administration on bone mineral content (BMC) in DEXA-induced osteoporosis in Wistar rats. Values were demonstrated as the mean  $\pm$  SEM (n = 10). values were analyzed by one-way ANOVA, then Tukey's post hoc analysis. P < 0.001 was established as significant. DEXA. L-C: L-Carnitine. DEXA: dexamethasone.

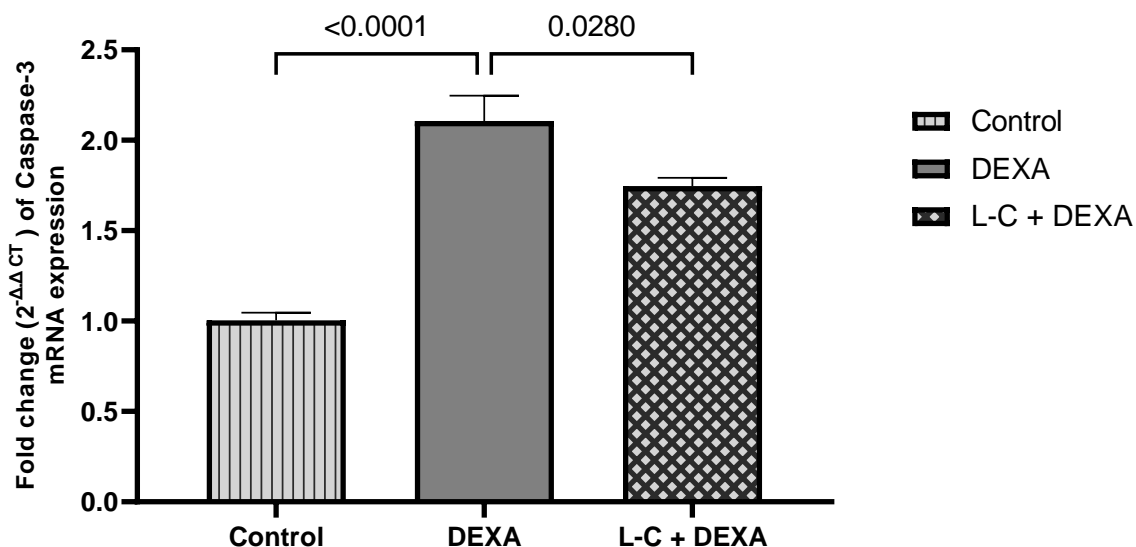


**Figure 5.** Effect of L-C administration on Caspase-3 gene expression in DEXA-induced osteoporosis in Wistar rats. Values were demonstrated as the mean  $\pm$  SEM (n = 10). values were analyzed by one-way ANOVA, then Tukey's post hoc analysis. P < 0.05 was established as significant. DEXA. L-C: L-Carnitine. DEXA: dexamethasone.

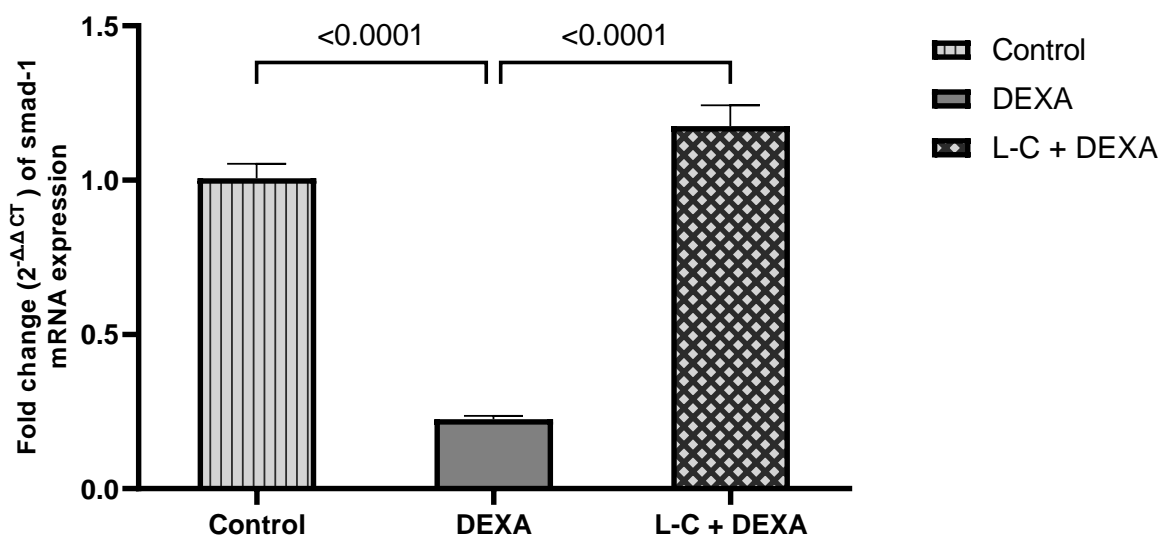


**Figure 6.** Effect of L-C administration on Smad-1 gene expression in DEXA-induced osteoporosis in Wistar rats. Values were demonstrated as the mean  $\pm$  SEM (n = 10). values were analyzed by one-way ANOVA, then Tukey's post hoc analysis. P < 0.001 was established as significant. DEXA. L-C: L-Carnitine. DEXA: dexamethasone.

### 3.11. Effect on autophagy-related gene (ATG) expression

DEXA therapy resulted in a substantial decrease (P<0.0001) in ATG mRNA gene expression as compared to the control groups. However, in comparison to DEX-treated groups, L-C administration in conjunction with DEXA resulted in significant advancement in the previously mentioned mRNA gene expression (P<0.0001), as

depicted in **Figure 7**.

### 3.12. Histopathological results

In the control group, the bone demonstrated unremarkable changes with abundant bone trabeculae (**Figures 8 A & B**). The bone was compacted and lamellated in thickness. They are relatively similar in shape and size. In bone trabeculae, several distributed functioning

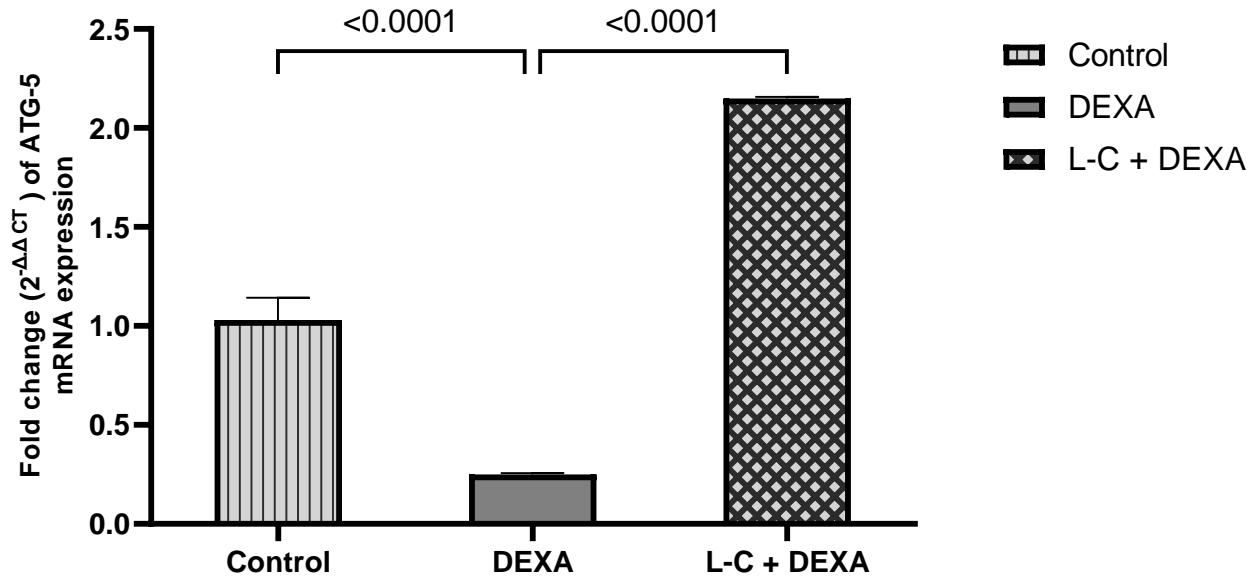


**Figure 7.** Effect of L-C administration on autophagy-related genes (ATG) expression in DEXA-induced osteoporosis in Wistar rats. Values were demonstrated as the mean  $\pm$  SEM (n = 10). values were analyzed by one-way ANOVA, then Tukey's post hoc analysis. P < 0.001 was established as significant. DEXA. L-C: L-Carnitine. DEXA: dexamethasone.

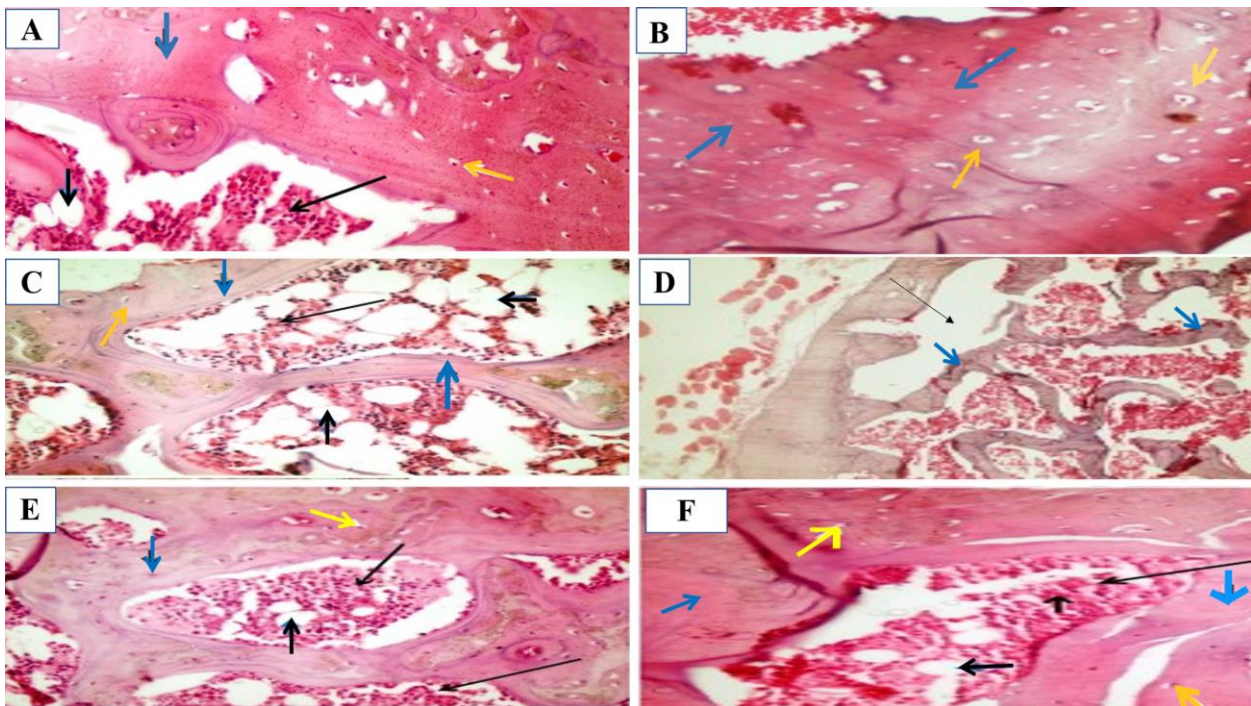


**Figure 8.** Effect of L-C administration on bone histopathology in DEXA-induced osteoporosis in Wistar rats.

**A & B:** photomicrographs of the femur of the control group revealed lamellated deep eosinophilic and thick bone trabeculae (blue arrows) with many osteocytes (yellow arrows). The trabeculae of bone were isolated by bone marrow (long black arrows) and a small number of fat cells (short black arrows).

**C & D:** photomicrographs of DEXA-treated rats (osteoporotic rats). The bone exhibited thin and pale eosinophilic trabeculae (blue arrows) associated with a small number of osteocytes (yellow arrows), broad bone marrow spaces (long black arrows) with abundant fat cell aggregates (short black arrows).

**E & F:** photomicrographs of femurs of (L-C+ DEXA) treated rats showed thick trabeculae (blue arrows), less extended bone marrow spaces (long black arrows), less fat cell aggregates (short black arrows), and more osteocytes (yellow arrows). H&E-stained section x 400 magnification.

osteocytes were observed. The hematopoietic cells in the bone marrow were preserved and not extended. The DEXA-treated group (osteoporotic rats) demonstrated bone resorption features (**Figures 8 C & D**). The bone appeared with pale color trabeculae, thin and asymmetrical in shape. The number of osteocytes was reduced, and the trabeculae were isolated by broadened bone marrow area, with an increased number of fat cells forming small aggregates.

L-C+DEXA treated group demonstrated relatively similar histological changes (**Figures 8 E & F**). The trabeculae of the bone are pale in color and thicker than the DEXA-treated group. The osteocytes are relatively increased in number. The spaces of the bone marrow are comparatively decreased and associated with fewer fat cells than the DEXA-treated group.

#### 4. Discussion

The majority of approved O.P therapies do not significantly reduce fracture risk and have numerous adverse effects (**Papaioannou et al., 2007**). Consequently, this study investigates novel target pathways unaffected by traditional medication, the L-C protective effects in response to DEXA-induced O.P in female Wistar rats in addition to investigating the role of autophagy, apoptosis, and oxidative stress, in the pathogenesis of O.P as well as the outcome of L-C.

The study findings demonstrated that DEXA administration led to a significant reduction in body weight, femur weight, and Seedor index, where administration of L-C before DEXA restored these parameters more or less near the control group values, which is consistent with the findings of (Filippopoulou et al., 2021). Seedor index is a bone density indicator; the higher the value, the denser the bone (**Mendes et al., 2006**). Some researchers attributed these effects to decreased cortical bone volume after DEXA treatment (**Filippopoulou et al., 2021**). Additional factors contributing to weight loss include appetite suppression and muscle atrophy, which limit protein synthesis and initiate protein breakdown (**Wu et al., 2018**). On the contrary, L-C administration produced a gain in body weight compared to the DEXA treated group and this is in harmony with **Mirzapor et al. (2016)** who explained their result through L-C induction of the oxidation of long-chain fatty acids and the increased level of acetyl coenzyme A in mitochondria, which increases the use of the protein

between oxidative stress and the development of O.P (**Polidori et al., 2001**). The negative impact of

diet by animals (**Mirzapor et al., 2016**). OPG is a soluble glycoprotein that interferes with RANKL-RANK binding, reducing osteoclast maturation and indirectly inhibiting bone resorption activity (**Guo et al., 2021**). In the present study, after comparison to the control group, 7 mg/kg/week of DEXA treatment for four successive weeks led to a considerable decrease in serum calcium, femoral BMD, BMC, and OPG with a substantial elevation in phosphorous and ALP levels, however, L-C supplementation ameliorated these effects. The histopathology of rat femurs also validated these findings, revealing thin and asymmetrical bone trabeculae, reduced numbers of osteocytes, and broadened bone marrow area compared to the control group, where L-C ameliorated these findings. These findings are compatible with earlier studies (**Cibulka et al., 2007; Hooshmand et al., 2008; Marcovina et al., 2013; Hozayen et al., 2016; Hachemi et al., 2018; Ahmed et al., 2022**).

**Hachemi et al. (2018)** attributed these effects to GIT and renal disturbance of calcium absorption by DEXA administration. In addition, DEXA induced free radical production resulting in hyperoxidant stress on osteoblast cells reducing their number and function (**El-Shenawy et al., 2013**). Moreover, the decrease in BMD and BMC can be attributed to DEXA via RANKL induction and reduction of OPG level (**Rauner et al., 2011**). In addition, **Canalis & Delany (2005)** attributed the previous findings to the inhibition of fibronectin and collagen productions along with stimulating collagenase synthesis after DEXA treatment which contributes to the decreased bone growth and thus decreased BMD and BMC. In contrast, Ferraretto and his colleagues demonstrated the ability of L-C to elevate calcium levels in vitro culture on human osteoblast-like cells (hOBs) and explained their result by two distinct pathways; the influx of calcium via the plasma membrane channels and a calcium discharge from internal stores (**Ferraretto et al., 2018**).

Furthermore, when compared to the control group, DEX treatment resulted in a significant elevation in oxidative stress markers such as MDA and NO as well as a significant reduction in TAC status. However, when compared to the osteoporotic group, L-C administration significantly improved the preceding parameters, which aligns with (**Murad, 2016; Terruzzi et al., 2019**).

Multiple studies have found a strong relationship

Smad promotes signal transduction in TGF- $\beta$  and BMP signaling pathways, which regulate both

DEX on oxidative stress may be due to the downregulation of the mRNA expression of CuZn-SOD and GSH-Px (Lv et al., 2018). Agidigbi & Kim (2019) reported that DEXA could induce osteoclast formation by stimulating mitochondrial dysfunction and elevating ROS production. On the other hand, the antioxidant effect of L-C is enhanced by its metal chelating capabilities of Fe<sup>+2</sup> and Cu<sup>+2</sup> (Surai, 2015). It also protects mitochondrial integrity in stressful situations and suppresses the generation of ROS (Sekine, 2017). In addition, Surai (2015) illustrated that L-Carnitine's antioxidant action is mediated by redox signaling, which involves Nrf2 and PPAR activation and NF- $\kappa$ B suppression, resulting in increased synthesis of antioxidant enzymes (SOD, GSH-Px, GR, GST, CAT).

Caspase 3 is involved in several biochemical apoptotic pathways, including the cleavage of nuclear and cytoplasmic substrates, chromatin condensation, DNA fragmentation, and the formation of apoptotic bodies (Salvesen & Dixit, 1997; Oruc et al., 2012; Pu et al., 2017).

The present study revealed that L-C ameliorated the apoptosis induced by DEXA treatment as indicated by the inhibition of caspase-3 gene expression, supported by the results of (Oruc et al., 2012; Moosavi et al., 2016; Deng et al., 2019; Kelek et al., 2019).

Deng et al. (2019) attributed the previous impacts via the DEXA-induced PI3K/AKT suppression and activation of GSK-3 $\beta$  in osteoblasts signaling pathway causing apoptosis (Deng et al., 2019). The ameliorating effect of L-C against apoptosis was detected in testicular tissues (Eid, 2016). L-C inhibits apoptosis via diminishing DEXA-induced oxidative stress, cytochrome c, and preserving cellular membranes by eliminating acetyl groups and free CoA (Fritz & Arrigoni-Martelli, 1993; Bodaghi-Namileh et al., 2018).

Autophagy promotes cell viability and survival by reducing the risk of deleterious protein aggregation. (Mameli et al., 2022). Autophagy may contribute to osteoporosis as it is involved in osteoblast survival and inhibiting oxidative stress-mediated osteoblast apoptosis (Li et al., 2017). In contrast, the inactivation of autophagy attenuates OPG-mediated osteoclast differentiation inhibition through the AMPK/mTOR/p70S6K signaling pathway (Tong et al., 2020).

osteoblast and osteoclast properties, and plays an essential role in bone remodeling regulation (Zou et al., 2021). Smad-1 deletion was found to increase P16 expression and shorten osteoblast's lifespan inducing osteoporosis (Kua et al., 2012).

In the current work, DEXA reduced autophagic markers, as evidenced by a decrease in ATG-5 in addition, it decreased the Smad-1 gene expression when compared to the control group. The co-administration of LC+ DEXA stimulated the ATG-5 and Smad-1 protein expression, which are consistent with (Tong et al., 2020; Tripathi et al., 2022). Jamali-Raeufy and colleagues found that a single dose of lipopolysaccharide decreased autophagic biomarkers such as the LC3 II/LC3 I ratio and becline-1, which was recovered by acetyl-L-C in a dose-dependent mechanism (Jamali-Raeufy et al., 2021). These results were postulated by the L-C initiation of Calcium/calmodulin-dependent protein kinase II (CaMKII) and extracellular signal-regulated kinase (ERKs/AKT) cascade by inducing the expression of osteogenic genes (Terruzzi et al., 2019). In addition, L-C can enhance the mitochondrial SOD synthesis while lowering ROS levels in osteoblasts, serving as a second messenger in gene down-regulation (Atashi et al., 2015). Moreover, L-C encourages the mRNA of ATG-1, lysosomal biogenesis-related genes, and phosphorylation of Bcl2 which is involved in the regulation of autophagy (Qiao et al., 2021).

These observations may be explained autophagy's capability to reduce ROS accumulation by facilitating the clearance of damaged mitochondria and activating antioxidant defense processes (Sadeghi et al., 2020).

## 5. Conclusion

According to the results of the present study, DEXA can cause O.P via various pathways, involving free radical accumulation, OPG pathway, apoptosis, smad-1 transcriptional factor, and autophagy. Furthermore, when combined with DEXA, L-C therapy demonstrated a significant protective effect and preserved bone mass.

In conclusion, L-C administration could be used as an adjunct in the management of osteoporotic bones, enhancing bone quality by stimulating autophagy and counteracting apoptosis and oxidative stress.

### Conflict of interest

The authors declare that there is no conflict of interest.

### Funding

This research did not receive any specific grant from funding agencies in the public, commercial, or not-for-profit sectors.

### Acknowledgments

The authors want to thank Dr. Sahar Gibril, lecturer of Histology, Faculty of Medicine, Sohag University, for her help in this study.

### References

- Abrahamsen, B. (2010). Adverse effects of bisphosphonates. *Calcified Tissue International*, 86(6), 421–435.
- Agidigbi, T. S., & Kim, C. (2019). Reactive Oxygen Species in Osteoclast Differentiation and Possible Pharmaceutical Targets of ROS-Mediated Osteoclast Diseases. *International Journal of Molecular Sciences*, 20(14), 3576.
- Ahmed, S. A., Abd El Reheem, M. H., & Elbahy, D. A. (2022). L-Carnitine ameliorates the osteoporotic changes and protects against simvastatin induced myotoxicity and hepatotoxicity in glucocorticoid-induced osteoporosis in rats. *Biomedicine & Pharmacotherapy*, 152, 113221.
- Atashi, F., Modarressi, A., & Pepper, M. S. (2015). The Role of Reactive Oxygen Species in Mesenchymal Stem Cell Adipogenic and Osteogenic Differentiation: A Review. *Stem Cells and Development*, 24(10), 1150–1163.
- Baek, K. H., Oh, K. W., Lee, W. Y., Lee, S. S., Kim, M. K., Kwon, H. S., Rhee, E. J., Han, J. H., Song, K. H., Cha, B. Y., Lee, K. W., & Kang, M. II. (2010). Association of oxidative stress with postmenopausal osteoporosis and the effects of hydrogen peroxide on osteoclast formation in human bone marrow cell cultures. *Calcified Tissue International*, 87(3), 226–235.
- Barnett, R. N., Ewing, N. S., & Skodon, S. B. (1976). Performance of “Kits” used for clinical chemical analysis of GOT (aspartate aminotransferase). *Clinical Biochemistry*, 9(C), 78–84.
- Beral, V. (2007). Ovarian cancer and hormone replacement therapy in the Million Women Study. *Lancet*, 369(9574), 1703–1710.
- Bernard, A., Rigault, C., Mazue, F., Borgne, F. Le, & Demarquoy, J. (2008). L-Carnitine Supplementation and Physical Exercise Restore Age-Associated Decline in Some Mitochondrial Functions in the Rat. *The Journals of Gerontology Series A: Biological Sciences and Medical Sciences*, 63(10), 1027–1033.
- Bodaghi-Namileh, V., Sepand, M. R., Omid, A., Aghsami, M., Seyednejad, S. A., Kasirzadeh, S., & Sabzevari, O. (2018). Acetyl-L-carnitine attenuates arsenic-induced liver injury by abrogation of mitochondrial dysfunction, inflammation, and apoptosis in rats. *Environmental Toxicology and Pharmacology*, 58, 11–20.
- Canalis, E., & Delany, E.M. (2005). Mechanisms of glucocorticoid action in bone. *Current Osteoporosis Reports*, 3(3), 98–102.
- Castelo-Branco, C. (1998). Management of Osteoporosis. *Drugs & Aging*, 12(Supplement 1), 25–32.
- Cawley, K. M., Bustamante-Gomez, N. C., Guha, A. G., MacLeod, R. S., Xiong, J., Gubrij, I., Liu, Y., Mulkey, R., Palmieri, M., Thostenson, J. D., Goellner, J. J., & O'Brien, C. A. (2020). Local Production of Osteoprotegerin by Osteoblasts Suppresses Bone Resorption. *Cell Reports*, 32(10), 108052.
- Cibulka, R., Racek, J., Pikner, R., Rajdl, D., Trefil, L., Vesela, E., Studenovska, M., & Siroka, R. (2007). Effect of L-carnitine supplementation on secondary hyperparathyroidism and bone metabolism in hemodialyzed patients. *Calcified Tissue International*, 81(2), 99–106.
- Clarke, B. L., & Khosla, S. (2010). Female reproductive system and bone. *Archives of Biochemistry and Biophysics*, 503(1), 118–128.
- Colucci, S., Mori, G., Vaira, S., Brunetti, G., Greco, G., Mancini, L., Simone, G. M., Sardelli, F., Koverech, A., Zallone, A., & Grano, M. (2005). L-carnitine and isovaleryl L-carnitine fumarate

positively affect human osteoblast proliferation and differentiation in vitro. *Calcified Tissue International*, 76(6), 458–465.

Daly, J. A., & Ertingshausen, G. (1972). Direct method for determining inorganic phosphate in serum with the “CentrifiChem”. *Clinical Chemistry*, 18(3), 263–265.

Deng, S., Dai, G., Chen, S., Nie, Z., Zhou, J., Fang, H., & Peng, H. (2019). Dexamethasone induces osteoblast apoptosis through ROS-PI3K/AKT/GSK3 $\beta$  signaling pathway. *Biomedicine & Pharmacotherapy*, 110, 602–608.

Ding, L.-Z., Teng, X., Zhang, Z.-B., Zheng, C.-J., & Chen, S.-H. (2018). Mangiferin inhibits apoptosis and oxidative stress via BMP2/Smad-1 signaling in dexamethasone-induced MC3T3-E1 cells. *International Journal of Molecular Medicine*, 41(5), 2517–2526.

Domazetovic, V., Marcucci, G., Iantomasi, T., Brandi, M. L., & Vincenzini, M. T. (2017). Oxidative stress in bone remodeling: Role of antioxidants. *Clinical Cases in Mineral and Bone Metabolism*, 14(2), 209–216.

Eid, A. (2016). Protective effect of L-carnitine against cisplatin-induced testicular toxicity in rats. *Al-Azhar Journal of Pharmaceutical Sciences*, 53(1), 123–142.

El-Shenawy, S., Yassin, N. A. Z., Badary, O. A., EL-Moneem, M. A., & AL-Shafeiy, H. M. (2013). Study of the effect of *Allium porrum* on osteoporosis induced in rats. *Der Pharmacia Lettre*, 5(1), 188-198.

Ferraretto, A., Bottani, M., Villa, I., Giusto, L., Signo, M., Senesi, P., Montesano, A., Vacante, F., Luzzi, L., Rubinacci, A., & Terruzzi, I. (2018). L-Carnitine activates calcium signaling in human osteoblasts. *Journal of Functional Foods*, 47, 270–278.

Filippopoulou, F., Habeos, G. I., Rinotas, V., Sophocleous, A., Sykiotis, G. P., Douni, E., & Chartoumpakis, D. V. (2021). Dexamethasone Administration in Mice Leads to Less Body Weight Gain over Time, Lower Serum Glucose, and Higher Insulin Levels Independently of NRF2. *Antioxidants*, 11(1), 4.

Fritz, I. B., & Arrigoni-Martelli, E. (1993). Sites of action of carnitine and its derivatives on the cardiovascular system: interactions with membranes. *Trends in Pharmacological Sciences*, 14(10), 355–360.

Galati, S., Boni, C., Gerra, M. C., Lazzaretti, M., & Buschini, A. (2019). Autophagy: a player in response to oxidative stress and DNA damage. *Oxidative Medicine and Cellular Longevity*, 2019, 5692958.

Guo, Y., Su, T., Yang, M., Li, C., Guo, Q., Xiao, Y., Huang, Y., Liu, Y., & Luo, X. (2021). The role of autophagy in bone homeostasis. *Journal of Cellular Physiology*, 236(6), 4152–4173.

Hachemi, Y., Rapp, A. E., Picke, A.-K., Weidinger, G., Ignatius, A., & Tuckermann, J. (2018). Molecular mechanisms of glucocorticoids on skeleton and bone regeneration after fracture. *Journal of Molecular Endocrinology*, 61(1), R75–R90.

Hooshmand, S., Balakrishnan, A., Clark, R. M., Owen, K. Q., Koo, S. I., & Arjmandi, B. H. (2008). Dietary l-carnitine supplementation improves bone mineral density by suppressing bone turnover in aged ovariectomized rats. *Phytomedicine*, 15(8), 595–601.

Hozayen, W. G., El-Desouky, M. A., Soliman, H. A., Ahmed, R. R., & Khaliefa, A. K. (2016). Antiosteoporotic effect of *Petroselinum crispum*, *Ocimum basilicum* and *Cichorium intybus* L. in glucocorticoid-induced osteoporosis in rats. *BMC Complementary and Alternative Medicine*, 16(1), 165.

Jamali-Raeufy, N., Alizadeh, F., Mehrabi, Z., Mehrabi, S., & Goudarzi, M. (2021). Acetyl-L-carnitine confers neuroprotection against lipopolysaccharide (LPS)-induced neuroinflammation by targeting TLR4/NF $\kappa$ B, autophagy, inflammation and oxidative stress. *Metabolic Brain Disease*, 36(6), 1391–1401.

Jiang, T., Ge, S., Shim, Y. H., Zhang, C., & Cao, D. (2015). Bone morphogenetic protein is required for fibroblast growth factor 2-dependent later-stage osteoblastic differentiation in cranial suture cells. *International Journal of Clinical and Experimental Pathology*, 8(3), 2946–2954.

- Kelek, S. E., Afşar, E., Akçay, G., Danişman, B., & Aslan, M. (2019). Effect of chronic L-carnitine supplementation on carnitine levels, oxidative stress and apoptotic markers in peripheral organs of adult Wistar rats. *Food and Chemical Toxicology*, 134, 110851.
- Koracevic, D., Koracevic, G., Djordjevic, V., Andrejevic, S., & Cosic, V. (2001). Method for the measurement of antioxidant activity in human fluids. *Journal of Clinical Pathology*, 54(5), 356–361.
- Kua, H.-Y., Liu, H., Leong, W. F., Li, L., Jia, D., Ma, G., Hu, Y., Wang, X., Chau, J. F. L., Chen, Y.-G., Mishina, Y., Boast, S., Yeh, J., Xia, L., Chen, G.-Q., He, L., Goff, S. P., & Li, B. (2012). c-Abl promotes osteoblast expansion by differentially regulating canonical and non-canonical BMP pathways and p16INK4a expression. *Nature Cell Biology*, 14(7), 727–737.
- Langenfeld, E. M., Kong, Y., & Langenfeld, J. (2006). Bone morphogenetic protein 2 stimulation of tumor growth involves the activation of Smad-1/5. *Oncogene*, 25(5), 685–692.
- Li, D. Y., Yu, J. C., Xiao, L., Miao, W., Ji, K., Wang, S. C., & Geng, Y. X. (2017). Autophagy attenuates the oxidative stress-induced apoptosis of Mc3T3-E1 osteoblasts. *Eur Rev Med Pharmacol Sci*, 21(24), 5548–5556.
- Li, H., Li, D., Ma, Z., Qian, Z., Kang, X., Jin, X., Li, F., Wang, X., Chen, Q., & Sun, H. (2018). Defective autophagy in osteoblasts induces endoplasmic reticulum stress and causes remarkable bone loss. *Autophagy*, 14(10), 1726–1741.
- Liu, Y., Ma, L., Yang, X., Bie, J., Li, D., Sun, C., Zhang, J., Meng, Y., & Lin, J. (2019). Menopausal Hormone Replacement Therapy and the Risk of Ovarian Cancer: A Meta-Analysis. *Frontiers in Endocrinology*, 10(3), 334–341.
- Lucinda, L. M. F., Vieira, B. J., Oliveira, T. T., Sá, R. C. S., Peters, V. M., Reis, J. E. P., & Guerra, M. O. (2010). Evidences of osteoporosis improvement in Wistar rats treated with Ginkgo biloba extract: A histomorphometric study of mandible and femur. *Fitoterapia*, 81(8), 982–987.
- Lv, Z., Peng, Y., Zhang, B., Fan, H., Liu, D., & Guo, Y. (2018). Glucose and lipid metabolism disorders in the chickens with dexamethasone-induced oxidative stress. *Journal of Animal Physiology and Animal Nutrition*, 102(2), e706–e717.
- Mameli, E., Martello, A., & Caporali, A. (2022). Autophagy at the interface of endothelial cell homeostasis and vascular disease. *The FEBS Journal*, 289(11), 2976–2991.
- Marcovina, S. M., Sirtori, C., Peracino, A., Gheorghide, M., Borum, P., Remuzzi, G., & Ardehali, H. (2013). Translating the basic knowledge of mitochondrial functions to metabolic therapy: Role of L-carnitine. *Translational Research*, 161(2), 73–84.
- Mendes, A. A., PAZ, I. C. L. A., Vulcano, L. C., Takahashi, S. E., García, R. G., Komiyama, C. M., & Balog, A. (2006). Bone mineral density and bone quality characteristics of broiler breeders. EPC 2006-12th European Poultry Conference, Verona, Italy, 10-14 September, 2006.
- Mirzapor, S. S., Salari, S., Mirzadeh, K., & Aghaei, A. (2016). Effect of different levels of vitamin c and L-carnitine on performance and some blood and immune parameters of broilers under heat stress. *Iranian Journal Of Animal Science Research*, 8(1), 141-153.
- Mizushima, N., & Levine, B. (2010). Autophagy in mammalian development and differentiation. *Nature Cell Biology*, 12(9), 823–830.
- Montaseri, A., Giampietri, C., Rossi, M., Riccioli, A., Del Fattore, A., & Filippini, A. (2020). The role of autophagy in osteoclast differentiation and bone resorption function. *Biomolecules*, 10(10), 1398.
- Moosavi, M., Rezaei, M., Kalantari, H., Behfar, A., & Varnaseri, G. (2016). L-carnitine protects rat hepatocytes from oxidative stress induced by T-2 toxin. *Drug and Chemical Toxicology*, 39(4), 445–450.
- Moustafa, A. M., & Boshra, V. (2011). The possible role of L-carnitine on the skeletal muscle of ovariectomized rats. *Journal of Molecular Histology*, 42(3), 217–225.
- Murad, H. A. S. (2016). L-carnitine, but not coenzyme q10, enhances the anti-osteoporotic effect of atorvastatin in ovariectomized rats.

Journal of Zhejiang University: Science B, 17(1), 43–53.

Ohkawa, H., Ohishi, N., & Yagi, K. (1979). Assay for lipid peroxides in animal tissues by thiobarbituric acid reaction. *Analytical Biochemistry*, 95(2), 351–358.

Oruc, E., kara, A., Can, I., karadeniz, A., & Simsek, N. (2012). Caspase-3 and CD68 Immunoreactivity in Lymphoid Tissues and Haematology of Rats Exposed to Cisplatin and L-carnitine. *Kafkas Universitesi Veteriner Fakultesi Dergisi*, 18(5), 871-878.

Papaioannou, A., Kennedy, C. C., Dolovich, L., Lau, E., & Adachi, J. D. (2007). Patient adherence to osteoporosis medications: Problems, consequences and management strategies. *Drugs and Aging*, 24(1), 37–55.

Pekala, J., Patkowska-Sokola, B., Bodkowski, R., Jamroz, D., Nowakowski, P., Lochynski, S., & Librowski, T. (2011). L-Carnitine - Metabolic Functions and Meaning in Humans Life. *Current Drug Metabolism*, 12(7), 667–678.

Polidori, M. C., Stahl, W., Eichler, O., Niestroj, I., & Sies, H. (2001). Profiles of antioxidants in human plasma. *Free Radical Biology and Medicine*, 30(5), 456–462.

Pu, X., Storr, S. J., Zhang, Y., Rakha, E. A., Green, A. R., Ellis, I. O., & Martin, S. G. (2017). Caspase-3 and caspase-8 expression in breast cancer: caspase-3 is associated with survival. *Apoptosis*, 22(3), 357–368.

Qiao, N., Chen, H., Du, P., Kang, Z., Pang, C., Liu, B., Zeng, Q., Pan, J., Zhang, H., Mehmood, K., Tang, Z., & Li, Y. (2021). Acetyl-L-Carnitine Induces Autophagy to Promote Mouse Spermatogonia Cell Recovery after Heat Stress Damage. *BioMed Research International*, 2021, 8871328.

Raisz, L. G. (2005). Pathogenesis of osteoporosis: Concepts, conflicts, and prospects. *Journal of Clinical Investigation*, 115(12), 3318–3325.

Rauner, M., Goettsch, C., Stein, N., Thiele, S., Bornhaeuser, M., De Bosscher, K., Haegeman, G., Tuckermann, J., & Hofbauer, L. C. (2011). Dissociation of Osteogenic and Immunological

Agonist, Compound A, in Human Bone Marrow Stromal Cells. *Endocrinology*, 152(1), 103–112.

Sadeghi, N., Erfani-Majd, N., Tavalae, M., Tabandeh, M. R., Drevet, J. R., & Nasr-Esfahani, M. H. (2020). Signs of ROS-associated autophagy in testis and sperm in a rat model of varicocele. *Oxidative Medicine and Cellular Longevity*, 2020, 5140383.

Salvesen, G. S., & Dixit, V. M. (1997). Caspases: Intracellular Signaling by Proteolysis. *Cell*, 91(4), 443–446.

Samelson, E. J., Broe, K. E., Demissie, S., Beck, T. J., Karasik, D., Kathiresan, S., & Kiel, D. P. (2008). Increased plasma osteoprotegerin concentrations are associated with indices of bone strength of the hip. *Journal of Clinical Endocrinology and Metabolism*, 93(5), 1789–1795.

Schmittgen, T. D., & Livak, K. J. (2008). Analyzing real-time PCR data by the comparative CT method. *Nature Protocols*, 3(6), 1101–1108.

Seedor, J. G., Quartuccio, H. A., & Thompson, D. D. (1991). The bisphosphonate alendronate (MK-217) inhibits bone loss due to ovariectomy in rats. *Journal of Bone and Mineral Research*, 6(4), 339–346.

Sekine, S. (2017). Mitochondrial proteolysis and its roles in stress responses. *Folia Pharmacologica Japonica*, 149(6), 264–268.

Surai, P. F. (2015). Antioxidant Action of Carnitine: Molecular Mechanisms and Practical Applications. *EC Veterinary Science*, 2(1), 66–84.

Suvarna, K. S., Layton, C., & Bancroft, J. D. (2018). Bancroft's theory and practice of histological techniques E-Book. Elsevier Health Sciences.

Terruzzi, I., Montesano, A., Senesi, P., Villa, I., Ferraretto, A., Bottani, M., Vacante, F., Spinello, A., Bolamperti, S., Luzi, L., & Rubinacci, A. (2019). L-Carnitine Reduces Oxidative Stress and Promotes Cells Differentiation and Bone Matrix Proteins Expression in Human Osteoblast-Like Cells. *BioMed Research International*, 2019, 5678548.

Tong, X., Zhang, C., Wang, D., Song, R., Ma, Y., Cao, Y., Zhao, H., Bian, J., Gu, J., & Liu, Z. (2020). Suppression of AMP-activated protein

## Effects by the Selective Glucocorticoid Receptor

kinase reverses osteoprotegerin-induced inhibition of osteoclast differentiation by reducing autophagy. *Cell Proliferation*, 53(1), e12714.

Tripathi, A. K., Rai, D., Kothari, P., Kushwaha, P., Sashidhara, K. V., & Trivedi, R. (2022). Benzofuran pyran hybrid prevents glucocorticoid induced osteoporosis in mice via modulation of canonical Wnt/ $\beta$ -catenin signaling. *Apoptosis*, 27(1–2), 90–111.

Wu, T., Yang, L., Jiang, J., Ni, Y., Zhu, J., Zheng, X., Wang, Q., Lu, X., & Fu, Z. (2018). Chronic glucocorticoid treatment induced circadian clock disorder leads to lipid metabolism and gut microbiota alterations in rats. *Life Sciences*, 192, 173–182.

Zhang, R., Liu, Z. G., Li, C., Hu, S. J., Liu, L., Wang, J. P., & Mei, Q. B. (2009). Du-Zhong (Eucommia ulmoides Oliv.) cortex extract prevent OVX-induced osteoporosis in rats. *Bone*, 45(3), 553–559.

Zou, M.-L., Chen, Z.-H., Teng, Y.-Y., Liu, S.-Y., Jia, Y., Zhang, K.-W., Sun, Z.-L., Wu, J.-J., Yuan, Z.-D., Feng, Y., Li, X., Xu, R.-S., & Yuan, F.-L. (2021). The Smad Dependent TGF- $\beta$  and BMP Signaling Pathway in Bone Remodeling and Therapies. *Frontiers in Molecular Biosciences*, 8, 389.

